# Adsorption of TNT, DNAN, NTO, FOX7, and NQ onto Cellulose, Chitin, and Cellulose Triacetate. Insights from Density Functional Theory Calculations

Guido Todde<sup>a,\*</sup>, Sanjiv K. Jha<sup>a</sup>, Gopinath Subramanian<sup>a</sup>, Manoj K. Shukla<sup>b</sup>

#### **Abstract**

Insensitive munitions (IM) compounds such as DNAN (2,4-dinitroanisole), NTO (3-nitro-1,2,4-triazol-5-one), NQ (nitroguanidine), and FOX7 (1,1-diamino-2,2dinitroethene) reduce the risk of accidental explosions due to shock and high temperature exposure. These compounds are being used as replacements for sensitive munition compounds such as TNT (2,4,6-trinitromethylbenzene) and RDX (1,3,5-hexahydro-1,3,5-trinitro-1,3,5-triazine). NTO and NQ in IM compounds are more soluble than TNT or RDX, hence they can easily spread in the environment and get dissolved if exposed to precipitation. DNAN solubility is comparable to TNT solubility. Cellulosic biomass, due to its abundance in the environment and its chemical structure, has a high probability of adsorbing these IM compounds, and thus, it is important to investigate the interactions between cellulose and cellulose like biopolymers (e.g. cellulose triacetate and chitin) with IM compounds. Using Density Functional Theory methods, we have studied the adsorption of TNT, DNAN, NTO, NQ, and FOX7 onto cellulose I $\alpha$  and I $\beta$ , chitin, and cellulose triacetate I (CTA I). Solvent effects on the adsorption were also investigated. Our results show that all contaminants are more strongly adsorbed onto chitin and cellulose Iα than onto CTA I and cellulose I $\beta$ . Dispersion forces were found to be the predominant contribution to

Email address: guido.todde@usm.edu (Guido Todde)

Preprint submitted to Surface Science

September 6, 2017

<sup>&</sup>lt;sup>a</sup> School of Polymers and High Performance Materials, University of Southern Mississippi, Hattiesburg, MS 39406, USA

<sup>&</sup>lt;sup>b</sup>Environmental Laboratory, Engineer Research and Development Center, Vicksburg, MS 39180, USA

<sup>\*</sup>Corresponding author

the adsorption energies of all contaminants.

*Keywords:* DFT, cellulose, TNT, DNAN, FOX7, insensitive munitions, adsorption

#### 1. Introduction

Armed forces around the world are developing and adopting insensitive munitions (IMs), that are designed to reduce the risk of unintentional detonation due to shock and high temperature exposure[1, 2]. Examples of IM compounds include DNAN (2,4-dinitroanisole), NTO (3-nitro-1,2,4-triazol-5one), NQ (nitroguanidine), and FOX7 (1,1-diamino-2,2-dinitroethene). These IM compounds have a lower risk of accidental detonation than TNT (2,4,6trinitromethylbenzene) or RDX (1,3,5-hexahydro-1,3,5-trinitro-1,3,5-triazine). IMs are produced with different formulations where either IM compounds or both the IM compounds and traditional compounds might be present in different ratio. The four IM compounds mentioned, viz. DNAN, NQ, NTO and FOX7, have a relatively higher solubility in water than TNT or RDX[3, 4, 5, 6, 7]. The production, storage, and usage of IMs may result in their dispersion in the environment. Moreover, due to their higher solubility, if IMs are exposed to precipitation they might be dissolved and the contamination can spread to groundwater and move off from its original location. Nevertheless, munitions containing compounds like TNT, RDX, and HMX are known to cause the same problem. The toxicity and impact on soil, water, and plants of explosives such as TNT and RDX has been studied in details[8, 9, 10, 11, 12, 13, 14]. IM compounds can be regarded as emerging new contaminants. Cellulosic biomass (like cellulose and chitin), due to its vast abundance in the environment, and its chemical structure, is very likely to interact with IM compounds. And thus, it is crucial to investigate the adsorption of IM compounds onto cellulose and cellulose derivatives. This investigation can help to understand the forces and interactions involved in the adsorption mechanisms of these compounds, and also serve as a starting point for the development of new materials intended

for remediation and detection technologies. Furthermore, due to the abundance of cellulose in the environment, the study of IM compounds adsorption onto cellulose will also help understanding the impact of these materials on the environment. Soil is also very likely to adsorb IM compounds, but IMs adsorption on soil is not within the scope of this study.

Cellulose is the most abundant biomaterial on earth as it is the main constituent of plants, and also found in bacteria, algae, and fungi[15]. Cellulose is a natural polymer formed by chains of  $\beta$ -D-glucanopyranose units linked by  $1\rightarrow 4$  glycosidic bonds[16, 17]. In its natural crystalline structure, cellulose can be found in two forms: I $\alpha$  and I $\beta$ [18]. The two allomorphs are not only found within the same cellulose sample[19], but also in the same microfibril[20]. The relative amounts of the two forms depend on the source. Ia is the most abundant form in the cell walls of algae and bacteria, while I $\beta$  is the most abundant form in wood, cotton, and ramie fibers[21, 22]. Cellulose can also crystallize in other forms, named cellulose II, III and IV. In cellulose II, which is obtained by regeneration or mercerization[23], glucan molecules run antiparallel. Cellulose III is obtained when either cellulose I or II is treated with liquid ammonia, the resulting allomorphs are called cellulose  $III_I$  or cellulose  $III_{II}$ respectively[24]. Heating of cellulose  $III_I$  or  $III_{II}$  produces cellulose  $IV_I$  and IV<sub>II</sub> respectively[25]. X-ray and neutron diffraction measurements[26, 27] have shown that cellulose I $\alpha$  crystallizes in a triclinic P1 unit cell containing one cellobiose molecule, while cellulose I $\beta$  has a monoclinic P2<sub>1</sub> unit cell containing two nonequivalent cellobiose molecules. In both allomorphs the chains of glucan molecules run in parallel forming sheets packed in a "parallel-up" fashion[26, 27]. Within the same sheet, the glucan molecules are held together by inter-chain hydrogen bonds formed between the hydroxylic groups. Adjacent sheets are held together by van der Waals dispersion forces[28].

Cellulose triacetate (CTA) is one of the most common derivatives of cellulose obtained by acetylation of cellulose fibers. CTA has many applications in the textile industry and is also used in the production of membranes and films. Depending on the acetylation procedure, two different polymorphs of CTA can be obtained. They are named CTA I and CTA II similarly to cellulose polymorphs, where in cellulose I chains run in a parallel fashion, while in cellulose II chains run antiparallel. CTA I is obtained by heterogeneous acetylation of cellulose I fibers[29]. Instead, CTA II can be obtained from either heterogeneous acetylation of cellulose II[30] or from homogeneous acetylation of cellulose I[31]. In CTA all cellulose hydroxyl groups are replaced by acetyl groups. The acetylation of hydroxyl groups increases the contact surface per glucose unit of CTA, which may results in the adsorption of larger quantity of contaminants. In its crystal structure, a monoclinic unit cell of CTA I is formed by a single polymer chain in a 2<sub>1</sub> helix conformation[31].

The second most abundant biopolymer on earth[32] is chitin, which is found in the exoskeleton of arthropods, and also in mollusks, algae, and fungi. Chitin is formed by  $\beta$ 1,4-linked units of acetyl-D-glucosamine. Chitin, like cellulose, is found in two forms:  $\alpha$  and  $\beta$ . The  $\alpha$ -form is the most common and in its crystal structure, the orthorhombic unit cell is formed by antiparallel chains in a 2<sub>1</sub> helix conformation[33, 34].

The adsorption of small molecules onto cellulose surfaces has been recently investigated by both experimental and theoretical groups. Several studies were focused on the adsorption of carbohydrates[35, 36, 37, 38], while other research groups studied the adsorption of aromatic compounds[39, 40, 41, 42], small proteins[43], and nanoparticles[44]. While Density Functional Theory (DFT) studies have shown that dispersion forces play a key role in the adsorption process and that they must be taken into account in order to correctly describe that the geometry and the energy of the complexes[37], a relatively small number of recent studies have included dispersion effects on the absorption of small molecules onto cellulosic surfaces[45, 46, 47].

In this article, we use DFT to compute the interaction energies of DNAN, NTO, NQ, FOX7, and TNT (see Figure 1) adsorbed onto cellulose (I $\alpha$  and I $\beta$ ), chitin, and cellulose triacetate I (100) surfaces. The interaction energies were calculated both in gas-phase and in water, and dispersion forces have been included.

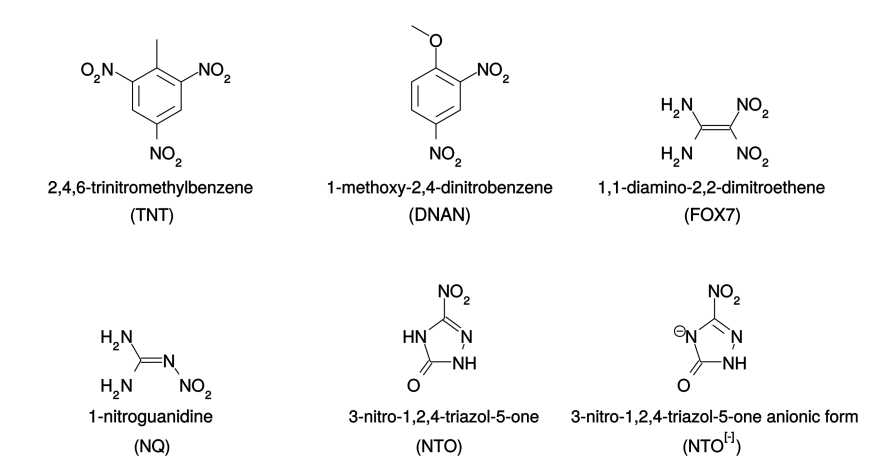


Figure 1: Schematic of the IM compounds along with their chemical names and abbreviations.

#### 2. Computational Methods

90

The model for both cellulose surfaces, I $\alpha$  (100) and I $\beta$  (100), are formed by two parallel strands of glucose tetraose (see Figure 2 and 3). Both cellulose models were built using the coordinates obtained from the crystallographic data of Nishiyama et al.[26, 27]. The model for the chitin surface is formed by two antiparallel chains containing four glucosamine units each, and was built using the coordinates obtained from the crystallographic data of Sikorski et al.[34]. The model for CTA I is formed by two parallel chains of glucose tetraose, where hydroxy groups on C2, C3, and C6 are acetylated (see Figure 2). The cellulose triacetate model was built using the coordinates obtained from the crystallographic data of Sikorski et al.[31]. In all models, the chains are terminated by attaching methoxy groups to atoms C1 and C4 (see Figure 2). The geometries of the surface models were optimized at the DFT[48, 49, 50, 51] level of theory using both B97D[52, 53, 54] functional with 6-31g basis set, and M06-2X[55] functional with 6-31g(d,p)[56, 57, 58, 59, 60, 61, 62, 63, 64, 65] basis set. The B97D and M06-2X functionals were chosen because they both include dispersion energy contributions, which are crucial interactions in the physisorption process. The 6-31g basis set was used to allow us to calculate the

zero point vibrational energies, since these calculations request large amount of memory. The surface models were built large enough to take into account all possible long range interactions with the adsorbates molecules. The models for the surface/contaminant complexes were built placing the contaminants at different locations (see Figure 3) on the optimized surfaces at a distance of approximately 4-5 Å. The complex structures were then optimized using the same functionals and basis set mentioned above. Single point calculations using the 6-31g(d,p) basis set were performed on all B97D/6-31g optimized geometries. The effect of bulk water solvation was modeled performing single point calculations on the optimized geometries using the CPCM approach[66, 67] with dielectric constant value equal to 80.0. The interaction energies of all complexes were corrected for basis set superposition error (BSSE) using the counterpoise correction scheme[68, 69].

The optimized geometries obtained at the B97D/6-31g level of theory were used to perform frequency calculations in order to estimate ZPVEs. The obtained ZPVE corrections (B97D/6-31g) were thereafter included in the interaction energies calculated with M06-2X/6-31g(d,p) and with B97D/6-31g(d,p). We have assumed that the ZPVE corrections do not vary significantly with the different functionals. The dispersion energy contribution to the electronic energy was calculated from the optimized geometries (with the B97D functional) through the D2 function developed by Grimme[53, 54] using the XYZ-Viewer software[70]. The number of atoms of the adsorbates and the surfaces are available in the Supporting Material (see Table S1). In order to avoid severe distortion of the surface models, the position of C2 and C5 atoms of all sugar rings were kept fixed during the optimization. All calculations were performed using the Gaussian09[71] software package.

The interaction energies ( $E_{int}$ ) between the contaminants and the different surfaces in gas phase and in water solution are obtained using the following

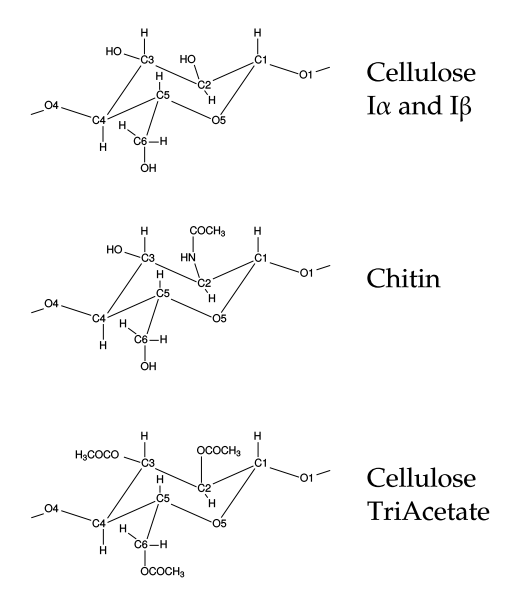


Figure 2: Schematic of the monomeric units of the surfaces, along with numbering of the atoms used in this paper.

# 135 formulae respectively:

$$E_{int(gas)} = E_{AB(gas)} - E_{A(gas)} - E_{B(gas)} + BSSE_{(gas)} + ZPVE_{(gas)}$$
(1)

$$E_{int(water)} = E_{AB(gas)} - E_{A(gas)} - E_{B(gas)} + BSSE_{(gas)} + ZPVE_{(gas)} + CPCM_{(water)}$$
(2)

where  $E_{AB(gas)}$ ,  $E_{A(gas)}$ , and  $E_{B(gas)}$  represent gas phase calculations of the electronic energy ( $E_{elec}$ ) of the complex (AB), the surface (A), and the contaminant (B) respectively.  $BSSE_{(gas)}$  is the basis set superposition error correction,  $ZPVE_{(gas)}$  is the zero-point vibrational energy correction, and  $CPCM_{(water)}$  is the bulk water solvation contribution.

# 3. Results and discussion

Of the different complex configurations used to start the geometry optimizations of each contaminant (see Figure 3), only the geometries with the

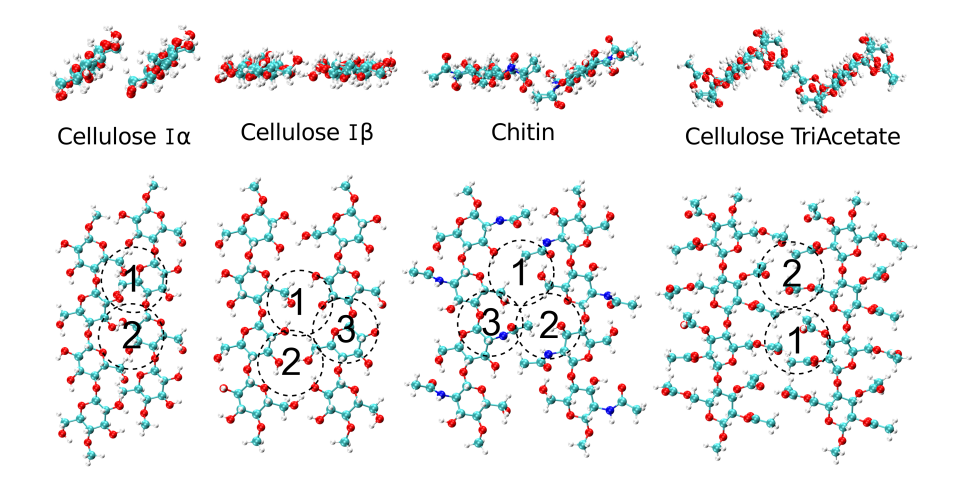


Figure 3: Surface models for cellulose  $I\alpha$ ,  $I\beta$ , chitin, and cellulose triacetate I. The top part of the figure shows the side view of the (100) surfaces, while the bottom part shows the top view. Circled numbers represent the starting position for all contaminants in the geometry optimization of the complexes. Atom colors scheme: C in cyan, O in red, N in blue, and H in white.

largest interaction energies will be discussed. In all optimized complexes, the contaminant was found adsorbed onto the same location over the biopolymer surfaces as revealed by both functionals, and the adsorption locations of the individual contaminants obtained with both functionals are reported in the Supporting Information (see Table S2). Since NTO is an acid with a  $pK_a$  value of 3.70-3.76[72, 73], its two forms, neutral and anionic, were investigated.

## 50 3.1. Cellulose Iα and Iβ

The calculated interaction energies of all contaminants with cellulose I $\alpha$  (100) and I $\beta$  (100) surfaces are presented in Table 1 for both gas phase and water solution. In both cases, gas phase and water solution, cellulose I $\alpha$  shows stronger  $E_{int}$  than I $\beta$  for all contaminants. The same trend was found with both functionals. The only exception is represented by NTO<sup>[-]</sup>, which shows a slightly larger  $E_{int}$  with cellulose I $\beta$  in aqueous solution (3-5 kcal/mol, depending on the functional). The anionic form of NTO is very unlikely to be found in the gas phase (where the neutral form is predominant), while in wa-

Table 1: Interaction Energies of TNT, DNAN, FOX7, NTO (in gas phase), NTO<sup>[-]</sup> (in water solution), and NQ adsorbed onto Cellulose I $\alpha$ , I $\beta$ , Chitin, and CTA I. All Energies Are Expressed in kcal/mol.

	Cell. Ια		Ce	Cell. I $\beta$		Chitin		CTA I	
	gas	water	gas	water	gas	water	gas	water	
	B97D								
TNT	-21.9	-13.5	-16.7	-10.1	-24.7	-11.6	-11.4	-5.1	
DNAN	-22.4	-11.3	-14.5	-10.2	-22.1	-7.2	-15.7	-7.4	
FOX7	-20.7	-9.2	-9.3	-2.6	-35.3	-12.7	-17.3	-7.2	
NTO	-19.4		-16.9		-23.7		-20.5		
$NTO^{[-]}$		-8.9		-13.5		-20.2		-4.1	
NQ	-25.0	-15.8	-16.9	-8.6	-31.7	-12.8	-17.4	-7.7	
	M06-2X								
TNT	-23.4	-13.2	-15.5	-8.4	-25.5	-11.6	-14.9	-9.3	
DNAN	-23.2	-10.8	-12.8	-8.2	-20.6	-6.5	-13.5	-7.2	
FOX7	-20.6	-8.5	-8.8	-2.2	-39.5	-16.9	-18.6	-8.5	
NTO	-21.6		-18.1		-24.7		-22.5		
$NTO^{[-]}$		-11.9		-11.3		-21.8		-3.3	
NQ	-24.9	-12.7	-18.2	-9.4	-28.8	-12.4	-17.5	-8.1	

Table 2: Dispersion Energy as a Percentage of Electronic Interaction Energies ( $E_{elec}$ ) of TNT, DNAN, FOX7, NTO, NTO<sup>[-]</sup>, and NQ adsorbed onto Cellulose I $\alpha$ , I $\beta$ , Chitin and CTA I.

	Cell. Ια	Cell. Ιβ	Chitin	CTA I			
	B97D						
TNT	71.8	98.1	79.0	84.0			
DNAN	70.9	93.6	73.5	90.0			
FOX7	52.2	87.9	49.3	72.0			
NTO	64.5	68.3	52.3	65.2			
$NTO^{[-]}$	35.1	30.1	26.0	53.6			
NQ	52.8	71.0	51.1	68.0			

ter, NTO<sup>[-]</sup> is the predominant form. Keeping this in mind, we can summarize that cellulose I $\alpha$  shows the strongest binding for all contaminants in gas phase. The same results are also found in water where NTO<sup>[-]</sup> represents the only exception as mentioned above.

While the two cellulose allomorphs, I $\alpha$  and I $\beta$ , are formed by the same glucan molecules, surfaces have different properties due to the mutual orientation of the glucan molecules. On the (100) surface of cellulose I $\alpha$ , the sheets are not parallel to the surface. The glucan molecules are tilted exposing the free hydroxyl groups, therefore the surface is hydrophilic[37]. On the flat (100) surface of cellulose I $\beta$ , the glucan molecules are arranged in a parallel fashion having the OH groups side by side forming interchain hydrogen bonds (see Figure 3). Hence, none of the hydroxyl groups are exposed and the resulting sheets are mainly hydrophobic[74].

When adsorption is driven by noncovalent interactions, there are four different components contribute to the total interaction energy[75]: electrostatics (between permanent multipoles), induction (between permanent and induced multipoles), dispersion (between instantaneous and induced multipoles) and Pauli repulsion (short-range interaction between electrons with same spin). Table 2 summarizes the dispersion energy as a percentage of the electronic in-

teraction energy ( $E_{elec}$ ) calculated with the B97D functional. Comparing the amount of dispersion energy with the  $E_{elec}$  of the complexes (see Table 2), we have found that in case of the hydrophobic surface of cellulose I $\beta$ , dispersion energy plays a predominant role. In fact, the amount of dispersion energy of cellulose I $\beta$  complexes is always at least 20% larger than that of the cellulose I $\alpha$  complexes. On the other hand, for the hydrophilic surface of cellulose I $\alpha$ , even though dispersion is still the predominant contribution to the interaction energy (>50%), the other three types of interaction become more significant.

In both the gas phase and in water, all contaminants have comparable interaction energies with cellulose I $\alpha$ . The same is also found for cellulose I $\beta$ , except for FOX7. The different interaction energies of FOX7 with the two cellulose surfaces depend mainly on the nature of the interaction. Hoja et~al. have shown that the dispersion contribution increases with the contact area between the surface and the adsorbate[37]. The molecular size of NQ and NTO is similar to FOX7 as is their dispersion energy when interacting with cellulose I $\beta$ . Nevertheless, the dispersion energy accounts for just the 70% of  $E_{elec}$  in case of NQ and NTO, while for FOX7 dispersion represents 90% of  $E_{elec}$ . Hence NQ and NTO form stronger interactions than FOX7 with cellulose I $\beta$  because for the former, interactions other than dispersion are more significant. On the other hand, TNT and DNAN exhibit stronger interactions with cellulose I $\beta$  than FOX7, even though they also have about 90% of their  $E_{elec}$  coming from dispersion. We believe that it is because of the larger molecular size of TNT and DNAN when compared with FOX7.

## 3.2. Cellulose Triacetate I

The  $E_{int}$  of all contaminants with CTA I are generally weaker than their complexes with cellulose I $\alpha$  both in gas phase and in water (see Table 2). NTO shows slightly stronger interactions with CTA I than cellulose I $\alpha$  in gas phase with both functionals. On the other hand, NTO<sup>[-]</sup> in water shows weaker interactions with CTA I than cellulose I $\alpha$ , moreover NTO<sup>[-]</sup> has the weakest interactions among all the contaminants with CTA I.

Comparison between CTA I and cellulose I $\beta$ , however, shows the opposite trend. Generally all contaminants forms stronger interactions with CTA I than cellulose I $\beta$  in gas phase, except TNT. TNT is found to have weaker or similar  $E_{int}$  with CTA I than cellulose I $\beta$  depending on the functional. In water the difference between the two surfaces become smaller. The only significant difference is found for NTO<sup>[-]</sup>, which binds more strongly to cellulose I $\beta$  than CTA I.

215

The structural difference between cellulose (both I $\alpha$  and I $\beta$ ) and CTA I is due to the acetylation of all hydroxyl groups in CTA I. When all OH groups of cellulose are replaced by acetyl groups to form CTA I, the resulting surface is found to be more hydrophobic. Moreover, the hydrophobicity of cellulose acetate increases with increasing acetylation[76]. The different hydrophobicity of cellulose I $\alpha$  and CTA I is at least partially due to the different possibility of the materials to form hydrogen bonds. Cellulose I $\alpha$  can form hydrogen bonds both as a donor (through the exposed OH groups) and as an acceptor (through O1, O4 and O5, see Figure 1). On the other hand, CTA I can only form hydrogen bonds as an acceptor, since all OH groups are replaced with acetyl groups. The different hydrophobicity of cellulose I $\alpha$  and CTA I is also manifested in the dispersion contribution to the  $E_{elec}$  (see Table 2). The amount of dispersion energy (as a percentage of the  $E_{elec}$ ) for the complexes with CTA I is closer to that of the complexes with cellulose  $I\beta$ , rather than that of the complexes with cellulose Ia. As mentioned above,  $NTO^{[-]}$  is found to bind more strongly to cellulose I $\beta$  than to CTA I. In this case, the negative charge imparts to NTO<sup>[-]</sup> the ability to form strong hydrogen bonds with the OH groups of cellulose I $\beta$  (see Supporting Information Figure S22). On the other hand, such strong hydrogen bonds can not be formed with CTA I due to the absence of hydroxyl groups. This is supported by the fact that for the NTO<sup>[-]</sup>/I $\beta$  complex, only 30% of the  $E_{elec}$  comes from dispersion while dispersion counts for about 54% of  $E_{elec}$  for the NTO<sup>[-]</sup>/CTA I complex.

### 3.3. Chitin

250

All contaminants adsorbed onto chitin show  $E_{int}$  (within 2-3 kcal/mol) similar to their complexes with cellulose I $\alpha$  in gas phase (see Table 2). Only FOX7 shows much stronger  $E_{int}$  (15-19 kcal/mol greater, depending on the functional) with chitin than with cellulose I $\alpha$ . We have found that all contaminants show generally higher or much higher affinity for chitin than for cellulose I $\beta$  or CTA I. The presence of exposed OH groups and acetylamino groups (bound on C2, see Figure 2) imparts to chitin the ability to form more hydrogen bonds than cellulose I $\beta$  or CTA I. Hence, the interactions between chitin and the contaminants are only partially due to dispersion. This is in contrast with the fact that dispersion forces are the main contribution to  $E_{elec}$  for cellulose I $\beta$  and CTA I. Furthermore, the complexes with chitin and cellulose I $\alpha$  show very similar dispersion contributions to the  $E_{elec}$ .

The  $E_{int}$  of chitin in water shows a different trend. The inclusion of solvent effects in the calculations decreases the difference in  $E_{int}$  between chitin and cellulose I $\alpha$ . TNT and NQ become more strongly bound to cellulose I $\alpha$  than to chitin. FOX7 and NTO<sup>[-]</sup> are still more strongly bound to chitin than to cellulose I $\alpha$ , but the difference in interaction energies between the two surfaces decreases significantly. DNAN, which showed stronger interactions with cellulose I $\alpha$  than chitin in gas phase, is still found to bind more strongly to cellulose I $\alpha$ . The same trend is found when comparing the  $E_{int}$  of IMs with chitin with that of cellulose I $\beta$  and CTA I. All contaminants still show higher affinity for chitin than the two other surfaces, but the difference in energy between chitin and cellulose I $\beta$  or CTA I decreases. In case of DNAN, the presence of water modifies the  $E_{int}$  in such a way that DNAN becomes more strongly bound to CTA I and cellulose I $\beta$  than to chitin.

The results obtained presented in this work are slightly different from one of our previous studies[77] on IMs adsorbed onto cellulose, as well as from a more comprehensive investigation on IMs adsorbed onto cellulose, CTA, chitin, and chitosan[78]. The differences in our findings are in part due to the different models used for the surfaces. In the present study, we have adopted

a larger surface model which should account for the wider contact area between adsorbent and adsorbate, but lesser interactions with side groups due to their involvement in interchain interactions stabilizing the bigger models considered in the present investigation. Jenkins *et al.*[79] have found that the cellulose triaceate filter adsorbs significant amounts of munition compounds such as HMX, RDX, TNT, and 2,4-DNT from water. In our recent investigation also[77] the CTA was found to remove significant amount of TNT and DNAN from the solution. Based upon the results of the present investigation, it appears that in those investigations the physical adsorption dominate where pore size and available surface play dominant role.

## 3.4. Electron Density Maps

A qualitative and visual description of the interactions between the contaminants and the surfaces can be obtained calculating an Electron Density Map Difference (EDMD). EDMDs are calculated by subtracting both the electron density of the adsorbate and the surface from the electron density of the complex. The resulting image (shown in Figure 4 for the complexes of chitin and CTA I with DNAN. For the EDMDs of all other complexes see Supporting Information) shows the differences in electron density generated by the interaction between the adsorbate and the surfaces. These differences are shown as regions where the electron density increases (yellow clouds in Figure 4) and regions where the electron density decreases (purple clouds in Figure 4). The solvent effect on the different surfaces can also be qualitatively evaluated from the EDMDs. Comparing the images in the second column (calculated in gas phase) with the images in the third column (calculated in water) of Figure 4, it is possible to see that the solvent weakens the interactions of DNAN with chitin more than it does with CTA I. As a general rule, looking at the EDMDs for all complexes, we see that the more hydrophilic a surface is the more its interactions with the contaminant are weakened.

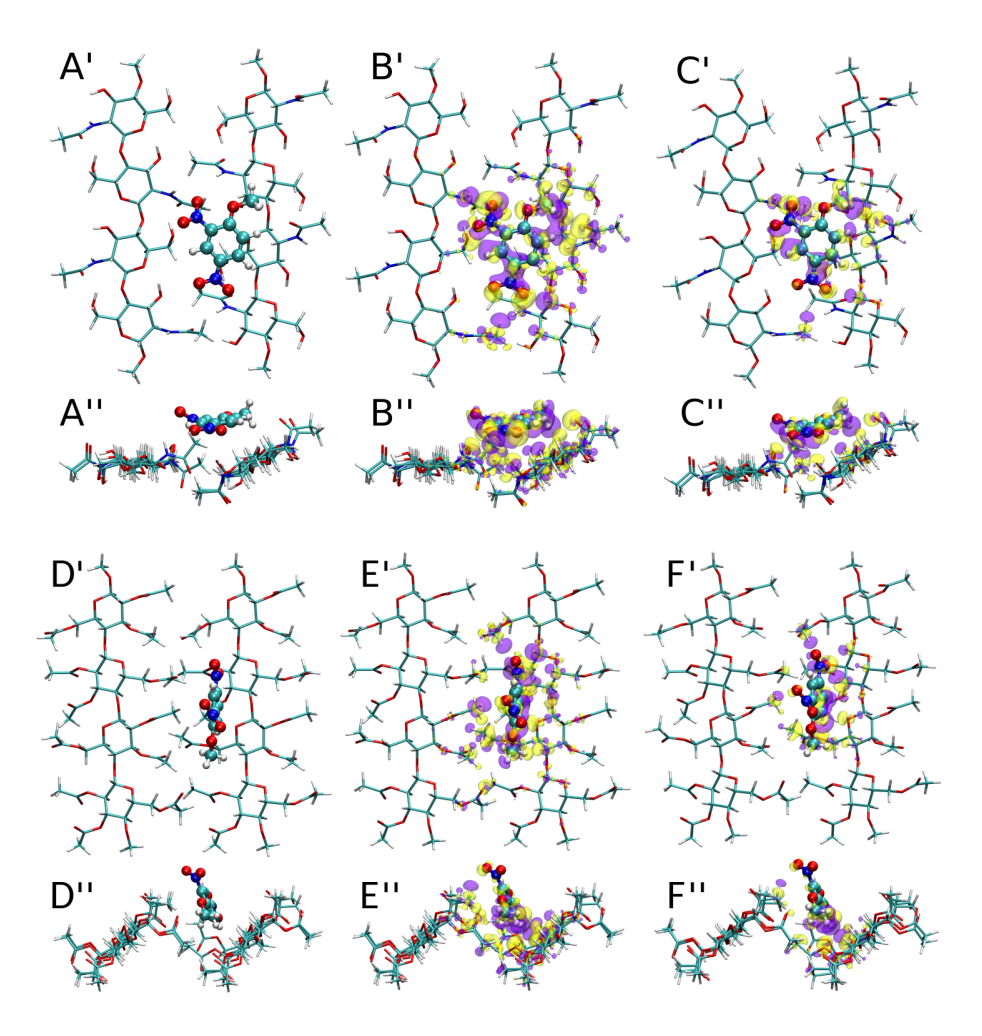


Figure 4: Electron Density Map Difference (EDMD) calculated for the adsorption of DNAN onto Chitin. EDMD isosurface value corresponds to  $0.0005~e/au^3$ . Yellow regions represent electron density gain, and purple regions represent electron density loss. A) and D) show the structure of the complexes of chitin and CTA I (shown in "licorice" representation) respectively, with DNAN (shown in "ball and stick"); B) and E) show the EDMD calculated in gas phase for chitin and CTA I respectively; C) and F) show the EDMD calculated in water for chitin and CTA I respectively. The symbols ' and " refer to top and side view of the surface plane respectively. Atom colors scheme: C in cyan, O in red, N in blue and H in white.

#### 4. Conclusions

We have studied the adsorption of different insensitive munition compounds, viz. DNAN, FOX7, NTO, NQ, and TNT onto two cellulose allomorphs (I $\alpha$  and I $\beta$ ), chitin, and CTA I. The investigation was carried out applying DFT methods and using two different functionals: B97D and M06-2X. Solvent effects were also included in our calculations. Dispersion energies are found to be the predominant contribution to the electronic interaction energy of all complexes. Moreover, the more hydrophobic the surface the more predominant the dispersion energies. CTA I and cellulose I $\beta$  complexes are found to have 15-30% higher contribution to their  $E_{elec}$  coming from dispersion energy than chitin or cellulose I $\alpha$ .

Of the different surfaces, cellulose I $\alpha$  and chitin show the strongest interactions with all contaminants both in gas phase and in water. In gas phase, chitin is found to be the strongest adsorption surface for almost all contaminants. The exception is DNAN, which has the largest  $E_{int}$  with cellulose I $\beta$  (2-3 kcal/mol more than chitin). In water, chitin was found to have similar  $E_{int}$  to cellulose I $\alpha$  for TNT and NQ, slightly weaker interactions for DNAN than all other surfaces and significantly stronger interactions for FOX7 and NTO<sup>[-]</sup> than all other surfaces. Chitin can be considered the strongest adsorbent for all contaminants considered in our study, with the exception of DNAN. Cellulose I $\alpha$  is found to be the strongest adsorbent for DNAN. Considering our results and the natural abundance of the different biopolymers, perhaps chitin has to be considered the best adsorbent overall. This is because chitin is the second most abundant biopolymer after cellulose, but as mentioned in the introduction, the I $\alpha$  allomorph is the most abundant in the wall cell of algae and bacteria while the I $\beta$  is the most abundant in wood, cotton, and ramie fibers.

#### Acknowledgements

G.T, S.K.J and G.S. acknowledge startup funds from the University of Southern Mississippi, and support form the U.S. Department of Defence via BAA-

16-0062. The use of trade, product, or firm name in this report is for descriptive purposes only and does not imply endorsement by the U.S. Government. The tests described and the resulting data presented herein, unless otherwise noted, were obtained from research conducted under the Environmental Quality Technology Program of the United States Army Corps of Engineers and the Environmental Security Technology Certification Program of the Department of Defense by the USAERDC. Permission was granted by the Chief of Engineers to publish this information. The findings of this report are not to be construed as an official Department of the Army position unless so designated by other authorized documents.

# 335 Supplementary Material

The Supplementary Material contain the interaction energies of all complexes calculated in both the gas phase and water solution, the adsorption location of all contaminants onto the different surfaces, and the EDMDs calculated for all complexes.

#### 340 References

345

- [1] D. R. Felt, J. L. Johnson, S. Larson, B. Hubbard, K. Henry, C. Nestler, J. H. Ballard, Evaluation of treatment technologies for wastewater from insensitive munitions production phase i: Technology down-selection, U.S. Army Engineer Research and Development Center, ERDC/EL TR-13-20, Vicksburg, USA (2013).
- [2] S. Taylor, E. Park, K. Bullion, K. Dontsova, Dissolution of three insensitive munitions formulations, Chemosphere 119 (2015) 342–348.
- [3] R. J. Spear, C. N. Louey, M. G. Wolfson, A Preliminary Assessment of 3-Nitro-1,2,4-Triazol-5-one (NTO) as an Insensitive High Explosive, Defence Science and Technology Organisation, Materials Research Laboratory, Maribyrnong, Australia, 1989.

- [4] W. R. Haag, R. Spanggord, T. Mill, R. T. Podoll, T.-W. Chou, D. S. Tse, J. C. Harper, Aquatic environmental fate of nitroguanidine, Environ. Toxicol. Chem. 9 (1990) 1359–1367.
- [5] J. M. Brannon, J. C. Pennington, Environmental fate and transport process descriptors for explosives, ERDC/EL TR-02-10 (2002).
  - [6] V. M. Boddu, K. Abburi, S. W. Maloney, R. Damavarapu, Thermophysical properties of an insensitive munitions compound, 2,4-dinitroanisole, J. Chem. Eng. Data 53 (2008) 1120–1125.
- [7] K. Dontsova, S. Taylor, B. M. Pesce-Rodriguez, R., J. Arthur, N. Mark, M. Walsh, J. Lever, J. Šimůnek, Dissolution of nto, dnan, and insensitive munitions formulations and their fates in soils, ERDC/CRREL TR-14-23 (2014).
- [8] R. G. Kuperman, R. T. Checkai, M. Simini, C. T. Phillips, J. E. Kolakowski, R. Lanno, Soil properties affect the toxicities of 2,4,6-trinitrotoluene (tnt) and hexahydro-1,3,5-trinitro-1,3,5-triazine (rdx) to the enchytraeid worm *Enchytraeus Crypticus*, Environ. Toxicol. Chem. 32 (2013) 2648–2659.
  - [9] G. Noctor, Lighting the fuse on toxic tnt, Science 349 (2015) 1052–1053.
- [10] E. J. Johnston, E. L. Rylott, E. Beynon, A. Lorenz, V. Chechik, N. C. Bruce, Monodehydroascorbate reductase mediates tnt toxicity in plants, Science 349 (2015) 1072–1075.
  - [11] E. A. Naumenko, B. Ahlemeyer, E. Baumgart-Vogt, Species-specific differences in peroxisome proliferation, catalase, and sod2 upregulation as well as toxicity in human, mouse, and rat hepatoma cells induced by the explosive and environmental pollutant 2,4,6-trinitrotoluene, Environ. Toxicol. 32 (2016) 989–1006.

[12] C. I. Olivares, R. Sierra-Alvarez, C. Alvarez-Nieto, L. Abrell, J. Chorover, J. A. Field, Microbial toxicity and characterization of

- dnan (bio)transformation product mixtures, Chemosphere 154 (2016) 499–506.
- [13] H. W. Schroer, K. L. Langenfeld, X. Li, H. J. Lehmler, C. L. Just, Biotransformation of 2,4-dinitroanisole by a fungul *Penicillium* sp., Biodegradation 28 (2017) 95–109.

- [14] A. J. Kennedy, A. R. Poda, N. L. Melby, L. C. Moores, S. M. Jordan, K. A. Gust, A. J. Bednar, Aquatic toxicity of photo-degraded insensitive munition 101 (imx-101) constituents, Environ. Toxicol. Chem.
  - [15] A. O'Sullivan, Cellulose: the structure slowly unravels, Cellulose 4 (1997) 173–207.
- [16] C. B. Purves, Chain Structure in Cellulose and Cellulose Derivatives: Part1, Ott and Spurlin Eds., Wiley-Interscience, New York, 1954.
  - [17] R. H. Marchessault, P. R. Sundararajan, Cellulose, in the Polysaccharides, Accademic Press, New York, 1983.
  - [18] R. H. Atalla, D. L. VanderHart, Native cellulose: a composite of two distinct crystalline forms, Science 223 (1984) 283–285.
- [19] J. Sugiyama, T. Okano, H. Yamamoto, F. Horii, Transformation of valonia cellulose crystals by an alkaline hydrothermal treatment, Macromolecules 23 (1990) 3196–3198.
  - [20] J. Sugiyama, R. Vuong, H. Chanzy, Electron diffraction study on the two crystalline phases occurring in native cellulose from an algal cell wall, Macromolecules 24 (1991) 4168–4175.
    - [21] F. Horii, A. Hirai, R. Kitamaru, Cp/mas carbon-13 nmr spectra on the crystalline components of native celluloses, Macromolecules 20 (1987) 2117–2120.

- [22] J. Sugiyama, J. Persson, H. Chanzy, Combined infrared and electron diffraction study of the polymorphism of native celluloses, Macromolecules 24 (1991) 2461–2466.
  - [23] A. J. Stipanovic, A. Sarko, Packing analysis of carbohydrates and polysaccharides. 6. molecular and crystal structure of regenerated cellulose ii, Macromolecules 9 (1976) 851–857.
- <sup>410</sup> [24] A. Sarko, J. Southwick, J. Hayashi, Packing analysis of carbohydrates and polysaccharides. 7. crystal structure of cellulose iii<sub>i</sub> adn its relationship to other cellulose polymorphs, Macromolecules 9 (1976) 857–863.
  - [25] E. S. Gardiner, A. Sarko, Packing analysis of carbohydrates and polysaccharides. 16. the crystal structure of celluloses  $iv_i$  and  $iv_{II}$ , Can. J. Chem. 63 (1985) 173–180.

- [26] Y. Nishiyama, P. Langan, H. Chanzy, Crystal structure and hydrogen bonding system in cellulose i $\beta$  from synchrotron x-ray and neutron fiber diffraction, J. Am. Chem. Soc. 124 (2002) 9074–9082.
- [27] Y. Nishiyama, J. Sugiyama, H. Chanzy, P. Langan, Crystal structure and hydrogen bonding system in cellulose i $\alpha$  from synchrotron x-ray and neutron fiber diffraction, J. Am. Chem. Soc. 125 (2003) 14300–14306.
  - [28] T. Shen, S. Gnanakaran, The stability of cellulose: a statistical perspective from a coarse-grained model of hydrogen-bond networks, Biophys. J. 96 (2009) 3032–3040.
- [29] B. S. Sprague, J. L. Riley, H. D. Noether, Factors influencing the crystal structure of cellulose triacetate, Text. Res. J. 28 (1958) 275–287.
  - [30] S. Watanabe, M. Takai, J. Hayashi, An x-ray study of cellulose triacetate, J. Polim. Sci. (C) 23 (1968) 825–830.
- [31] P. Sikorski, M. Wada, L. Heux, H. Shintani, B. T. Stokke, Crystal structure of cellulose triacetate i, Macromolecules 37 (2004) 4547–4553.

- [32] R. Taranathan, F. Kittur, Chitin the undisputed biomolecule of great potential, Crit. Rev. Food Sci. Nutr. 43 (2003) 61–87.
- [33] R. Minke, J. Blackwell, The structure of  $\alpha$ -chitin, J. Mol. Biol. 120 (1978) 167–181.
- [34] P. Sikorski, R. Hori, M. Wada, Revisit of α-chitin crystal structure using high resolution x-ray diffraction data, Macromolecules 10 (2009) 1100– 1105.
  - [35] J. Hanus, K. Mazeau, The xyloglucan-cellulose assembly at the atomic scale, Biopolymers 82 (2006) 59–73.
- [36] M. Bergenstråhle, J. Wohlert, M. E. Himmel, J. W. Brady, Simulation studies of the insolubility of cellulose, Carbohydr. Res. 345 (2010) 2060–2066.
  - [37] J. Hoja, R. J. Maurer, A. F. Sax, Adsorption of glucose, cellobiose, and cellotetraose onto cellulose model surfaces, J. Phys. Chem. B 118 (2014) 9017–9027.
- [38] Z. Zhao, V. H. Crespi, J. D. Kubicki, D. J. Cosgrove, L. Zhong, Molecular dynamics simulation study of xyloglucan adsorption on cellulose surfaces: Effects of surface hydrophobicity and side-chain variation, Cellulose 21 (2014) 1025–1039.
  - [39] K. Mazeau, C. Vergelati, Atomistic modeling of the adsorption of benzophenone onto cellulose surfaces, Langmuir 18 (2002) 1919–1927.

- [40] D. Da Silve Perez, R. Ruggiero, L. C. Morais, A. E. H. Machado, K. Mazeau, Theoretical and experimental studies on the adsorption of aromatic compounds onto cellulose, Langmuir 20 (2004) 3151–3158.
- [41] K. Mazeau, M. Wyszomirski, Modelling of congo red adsorption on the hydrophobic surface of cellulose using molecular dynamics, Cellulose 19 (2012) 1495–1506.

- [42] K. Mazeau, L. Charlier, The molecular basis of the adsorption of xylans on cellulose surface, Cellulose 19 (2012) 337–349.
- [43] M. R. Nimlos, G. T. Beckham, J. F. Matthews, L. Bu, M. E. Himmel, M. F. Crowley, Binding preferences, surface attachment, diffusivity, and orientation of a family 1 carbohydrate-binding module on cellulose, J. Biol. Chem. 287 (2012) 20603–20612.
  - [44] T. Nypelö, H. Pynnönen, M. Österberg, J. Paltakari, J. Laine, Interactions between inorganic nanoparticles and cellulose nanofibrils, Cellulose 19 (2012) 779–792.

- [45] Y. Li, M. Lyn, J. W. Davenport, Ab initio studies of cellulose i: Crystal structure, intermoleculear forces, and interactions with water, J. Phys. Chem. C 115 (2011) 11533–11539.
- [46] P. Bourassa, J. Bouchard, S. Robert, Quantum chemical calculations of pristine and modified crystalline cellulose surfaces: Benchmarking interactions and adsorption of water and electrolyte, Cellulose 21 (2014) 71–86.
  - [47] J. D. Kubicki, H. D. Watts, Z. Zhao, L. Zhong, Quantum mechanical calculations on cellulose-water interactions: Structures, energetics, vibrational frequencies and nmr chemical shifts for surfaces of  $i\alpha$  and  $i\beta$  cellulose, Cellulose 21 (2014) 909–926.
  - [48] K. W. Hohenberg P., Inhomogeneous Electron Gas, Phys. Rev. B 136 (1964) 864–871.
  - [49] S. L. J. Kohn W., Self-Consistent Equations Including Exchange and Correlation Effects, Phys. Rev. A 140 (1951) (1965) 1133–1138.
- [50] R. G. Parr, W. Yang, Density-Functional Theory of Atoms and Molecules, Oxford University Press.
  - [51] D. R. Salahub, Z. C. Zerner, The Challenge of d and f Electrons, ACS, Washington, D.C.

- [52] A. D. Becke, Density-functional thermochemistry. v. systematic optimization of exchange-correlation functionals, J. Chem. Phys. 107 (1997) 8554–8560.
  - [53] S. Grimme, Semiempirical gga-type density functional constructed with a long-range dispersion correction, J. Comp. Chem. 27 (2006) 1787–1799.
  - [54] T. Schwabe, S. Grimme, Double-Hybrid Density Functionals with Long-Range Dispersion Corrections: Higher Accuracy and Extended Applicability., Phys. Chem. Chem. Phys. 9 (2007) 3397–406.

- [55] Y. Zhao, D. G. Truhlar, The m06 suite of density functionals for main group thermochemistry, thermochemical kinetics, noncovalent interactions, excited states, and transition elements: Two new functionals and systematic testing of four m06-class functionals and 12 other functionals, Theor. Chem. Acc. 120 (2008) 215–241.
- [56] R. Ditchfield, W. J. Hehre, J. A. Pople, Self-consistent molecular orbital methods. 9. extended gaussian-type basis for molecular-orbital studies of organic molecules, J. Chem. Phys. 54 (3) (1971) 724–728.
- [57] W. J. Hehre, R. Ditchfield, J. A. Pople, Self-consistent molecular orbital methods. 12. further extensions of gaussian-type basis sets for use in molecular-orbital studies of organic-molecules, J. Chem. Phys. 56 (3) (1972) 2257–2262.
- [58] P. C. Hariharan, J. A. Pople, Influence of polarization functions on molecular-orbital hydrogenation energies, Theor. Chem. Acc. 28 (3) (1973) 213–222.
  - [59] P. C. Hariharan, J. A. Pople, Accuracy of ah<sub>n</sub> equilibrium geometries by single determinant molecular-orbital theory, Mol. Phys. 27 (3) (1974) 209–214.
- [60] M. S. Gordon, The isomers of silacyclopropane, Chem. Phys. Lett. 76 (3) (1980) 163–168.

[61] M. M. Francl, W. J. Pietro, W. J. Hehre, J. S. Binkley, D. J. DeFrees, J. A. Pople, M. S. Gordon, Self-consistent molecular orbital methods. 23. a polarization-type basis set for 2nd-row elements, J. Chem. Phys. 77 (3) (1982) 3654–3665.

515

520

- [62] R. C. J. Binning, L. A. Curtiss, Compact contracted basis-sets for 3rd-row atoms ga-kr, J. Comp. Chem. 11 (3) (1990) 1206–1216.
- [63] J. P. Blaudeau, M. P. McGrath, L. A. Curtiss, L. Radom, Extension of gaussian-2 (g2) theory to molecules containing third-row atoms k and ca, J. Chem. Phys. 107 (3) (1997) 5016–5021.
- [64] V. A. Rassolov, J. A. Pople, M. A. Ratner, T. L. Windus, 6-31g\* basis set for atoms k through zn, J. Chem. Phys. 109 (3) (1998) 1223–1229.
- [65] V. A. Rassolov, M. A. Ratner, J. A. Pople, P. C. Redfern, L. A. Curtiss, 6-31g\* basis set for third-row atoms, J. Comp. Chem. 22 (3) (2001) 976–984.
- [66] V. Barone, M. Cossi, Quantum calculation of molecular energies and energy gradients in solution by a conductor solvent model, J. Phys. Chem. A 102 (1998) 1995–2001.
  - [67] M. Cossi, N. Rega, G. Scalmani, V. Barone, Energies, structures, and electronic properties of molecules in solution with the c-pcm solvation model, J. Comp. Chem 24 (2003) 669–681.
  - [68] S. F. Boys, F. Bernardi, Calculation of small molecular interactions by differences of separate total energies - some procedures with reduced errors, Mol. Phys. 19 (1970) 553.
- [69] S. Simon, M. Duran, J. J. Dannenberg, How does basis set superposition error change the potential surfaces for hydrogen bonded dimers?, J. Chem. Phys. 105 (1996) 11024–11031.
  - [70] S. De Marothy, XYZ-viewer, version 0.970, Stockholm, 2010.

- [71] M. J. Frisch, G. W. Trucks, H. B. Schlegel, G. E. Scuseria, M. A. Robb, J. R. Cheeseman, G. Scalmani, V. Barone, B. Mennucci, G. A. Petersson, H. Nakatsuji, M. Caricato, X. Li, H. P. Hratchian, A. F. Izmaylov, J. Bloino, 540 G. Zheng, J. L. Sonnenberg, M. Hada, M. Ehara, K. Toyota, R. Fukuda, J. Hasegawa, M. Ishida, T. Nakajima, Y. Honda, O. Kitao, H. Nakai, T. Vreven, J. A. Montgomery, Jr., J. E. Peralta, F. Ogliaro, M. Bearpark, J. J. Heyd, E. Brothers, K. N. Kudin, V. N. Staroverov, R. Kobayashi, J. Normand, K. Raghavachari, A. Rendell, J. C. Burant, S. S. Iyengar, 545 J. Tomasi, M. Cossi, N. Rega, J. M. Millam, M. Klene, J. E. Knox, J. B. Cross, V. Bakken, C. Adamo, J. Jaramillo, R. Gomperts, R. E. Stratmann, O. Yazyev, A. J. Austin, R. Cammi, C. Pomelli, J. W. Ochterski, R. L. Martin, K. Morokuma, V. G. Zakrzewski, G. A. Voth, P. Salvador, J. J. Dannenberg, S. Dapprich, A. D. Daniels, . Farkas, J. B. Foresman, J. V. Ortiz, 550 J. Cioslowski, D. J. Fox, Gaussian 09 Revision B.01Gaussian Inc. Wallingford CT 2009.
  - [72] G. I. Chipen, R. P. Bokalder, V. Y. Grinstein, 1,2,4-triazol-3-one and its nitro and amino derivatives, Chem. Heterocycl. Compd. 2 (1966) 110–116.
- [73] L. Le Campion, M. T. Adeline, J. Ouazzani, Separation of nto related 1,2,4-triazole-3-one derivatives by a high performance liquid chromatography and capillary electrophoresis, Propellants Explos. Pyrotech. 22 (1997) 233–237.
- [74] K. Mazeau, A. Rivet, Wetting the (110) and (100) surfaces of  $i\beta$  cellulose studied by molecular dynamics, Biomacromolecules 9 (2008) 1352–1354.
  - [75] A. Stone, The Theory of Intermolecular Forces, 2nd ed., Oxford Press, Oxford, U.K., 2013.
  - [76] M. Lewin, E. M. Pearce, Handbook of Fiber Chemistry, 2nd Edition, Revised and Expanded, Marcel Dekker Inc., New York, USA, 1998.
- [77] M. K. Shukla, A. Poda, Adsorption of emerging munitions contaminants

- on cellulose surface a combined theoretical and experimental investigation, Bull. Environ. Contam. Toxicol. 96 (2016) 784–790.
- [78] L. A. Gurtowski, C. S. Griggs, V. G. Gude, M. K. Shukla, An integrated theoretical and experimental investigation of insensitive munition compounds adsorption on cellulose, cellulose triacetate, chitin and chitosan, To be published.

[79] T. F. Jenkins, L. K. Knapp, M. E. Walsh, Losses of explosive residues on disposable membrane filters, Technical Report, Accession Number ADA 180889 (1987).

